

## PHAGOCYTES, GRANULOCYTES, AND MYELOPOIESIS

## Pharmacological targeting of plasmin prevents lethality in a murine model of macrophage activation syndrome

Hiroshi Shimazu,<sup>1,2</sup> Shinya Munakata,<sup>1</sup> Yoshihiko Tashiro,<sup>1</sup> Yousef Salama,<sup>2</sup> Douaa Dhahri,<sup>2</sup> Salita Eiamboonsert,<sup>2</sup> Yasunori Ota,<sup>3</sup> Haruo Onoda,<sup>3</sup> Yuko Tsuda,<sup>4</sup> Yoshio Okada,<sup>4</sup> Hiromitsu Nakachi,<sup>1</sup> Beate Heissig,<sup>2,5,\*</sup> and Koichi Hattori<sup>1,6,\*</sup>

<sup>1</sup>Center for Stem Cell Biology and Regenerative Medicine, <sup>2</sup>Division of Stem Cell Dynamics, Center for Stem Cell Biology and Regenerative Medicine, and <sup>3</sup>Department of Diagnostic Pathology, The Institute of Medical Science, The University of Tokyo, Tokyo, Japan; <sup>4</sup>Faculty of Pharmaceutical Sciences, Kobe Gakuin University, Kobe, Japan; and <sup>5</sup>Atopy Center and <sup>6</sup>Center for Genome and Regenerative Medicine, Juntendo University School of Medicine, Tokyo, Japan

## Key Points

- Plasminogen/plasmin is excessively activated in the murine model of fulminant MAS.
- The genetic or pharmacological inhibition of plasminogen/plasmin counteracted a cytokine storm and tissue damage in fulminant MAS.

**Macrophage activation syndrome (MAS) is a life-threatening disorder characterized by a cytokine storm and multiorgan dysfunction due to excessive immune activation. Although abnormalities of coagulation and fibrinolysis are major components of MAS, the role of the fibrinolytic system and its key player, plasmin, in the development of MAS remains to be solved. We established a murine model of fulminant MAS by repeated injections of Toll-like receptor-9 (TLR-9) agonist and D-galactosamine (DG) in immunocompetent mice. We found plasmin was excessively activated during the progression of fulminant MAS in mice. Genetic and pharmacological inhibition of plasmin counteracted MAS-associated lethality and other related symptoms. We show that plasmin regulates the influx of inflammatory cells and the production of inflammatory cytokines/chemokines. Collectively, our findings identify plasmin as a decisive checkpoint in the inflammatory response during MAS and a potential novel therapeutic target for MAS. (Blood. 2017;130(1):59-72)**

## Introduction

Macrophage activation syndrome (MAS) is a hyperinflammatory state with high mortality. MAS patients show signs of prolonged fever, pancytopenia, hepatosplenomegaly, hyperferritinemia, hypertriglyceridemia, liver dysfunction, coagulopathy, and hemophagocytosis. MAS is clinically linked to hemophagocytic lymphohistiocytosis syndrome (HLH) and hemophagocytic syndrome (HPS), and is characterized by an acute episode of severe overshooting inflammation and the activation and expansion of macrophages. An excess of activated macrophages and lymphocytes produces high levels of tumor necrosis factor- $\alpha$  (TNF- $\alpha$ ), interferon- $\gamma$  (IFN- $\gamma$ ), and interleukin-6 (IL-6), which leads to multiorgan failure and high mortality.<sup>1,2</sup> The cytokine storm drives the systemic inflammatory humoral and cellular response, and generates imbalances between coagulation and fibrinolysis. Key molecular players of the coagulation cascade like tissue factor, thrombin, and fibrinogen are linked with the inflammatory response. Plasmin activation occurs in the acute phase of inflammation and is associated with enhanced macrophage influx into inflamed tissues.<sup>3,4</sup> Activated macrophages produce increased levels of plasminogen activator leading to hyperfibrinolysis in MAS.<sup>5</sup> Plasmin, a key enzyme of the fibrinolytic cascade, can degrade fibrin clots. However, other roles of fibrinolytic factors like plasmin in MAS are not well understood.

Plasmin can activate other proteases like matrix metalloproteinases (MMPs) by cleavage of inactive precursors to form the active enzymes.<sup>6-8</sup> Plasma TNF- $\alpha$ , Fas-ligand (Fas-L), and soluble IL-2 receptor levels were elevated in the active phase of MAS.<sup>9-11</sup> Shedding of these cytokines can be catalyzed by several MMPs.<sup>12</sup> Plasminogen/plasmin can induce the transcription of TNF- $\alpha$ , IL-1, IL-6, and CCL2<sup>13-18</sup> by activating NF- $\kappa$ B, and can modify macrophage migration.<sup>17-20</sup> Lipopolysaccharide-challenged IL-6 transgenic mice showed features typically present in MAS patients,<sup>21</sup> demonstrating that active inflammation contributes to the development of MAS.

Given that anticytokine therapeutics like anti-TNF- $\alpha$  and anti-IL-1 agents are effective against therapy-resistant MAS,<sup>22-31</sup> and plasmin regulates the inflammatory response, we hypothesized that plasmin could be a novel therapeutic target for MAS.

We investigate the role of fibrinolytic factors in a murine model of MAS. It was reported that repeated Toll-like receptor (TLR) TLR-9 stimulation by its ligand cytosine guanine dinucleotide [CpG]-oligodeoxynucleotide 1826 (ODN1826) (henceforth termed CpG) resulted in a MAS-like disease in immunocompetent mice. One drawback of this model was that although typical MAS symptoms could be observed, no lethality was observed. This is in contrast to the high death rate in patients with fulminant HLH/HPS.<sup>32</sup> D-galactosamine

Submitted 6 September 2016; accepted 10 March 2017. Prepublished online as *Blood* First Edition paper, 21 March 2017; DOI 10.1182/blood-2016-09-738096.

\*B.H. and K.H. share senior authorship.

The online version of this article contains a data supplement.

There is an Inside *Blood* Commentary on this article in this issue.

The publication costs of this article were defrayed in part by page charge payment. Therefore, and solely to indicate this fact, this article is hereby marked "advertisement" in accordance with 18 USC section 1734.

© 2017 by The American Society of Hematology

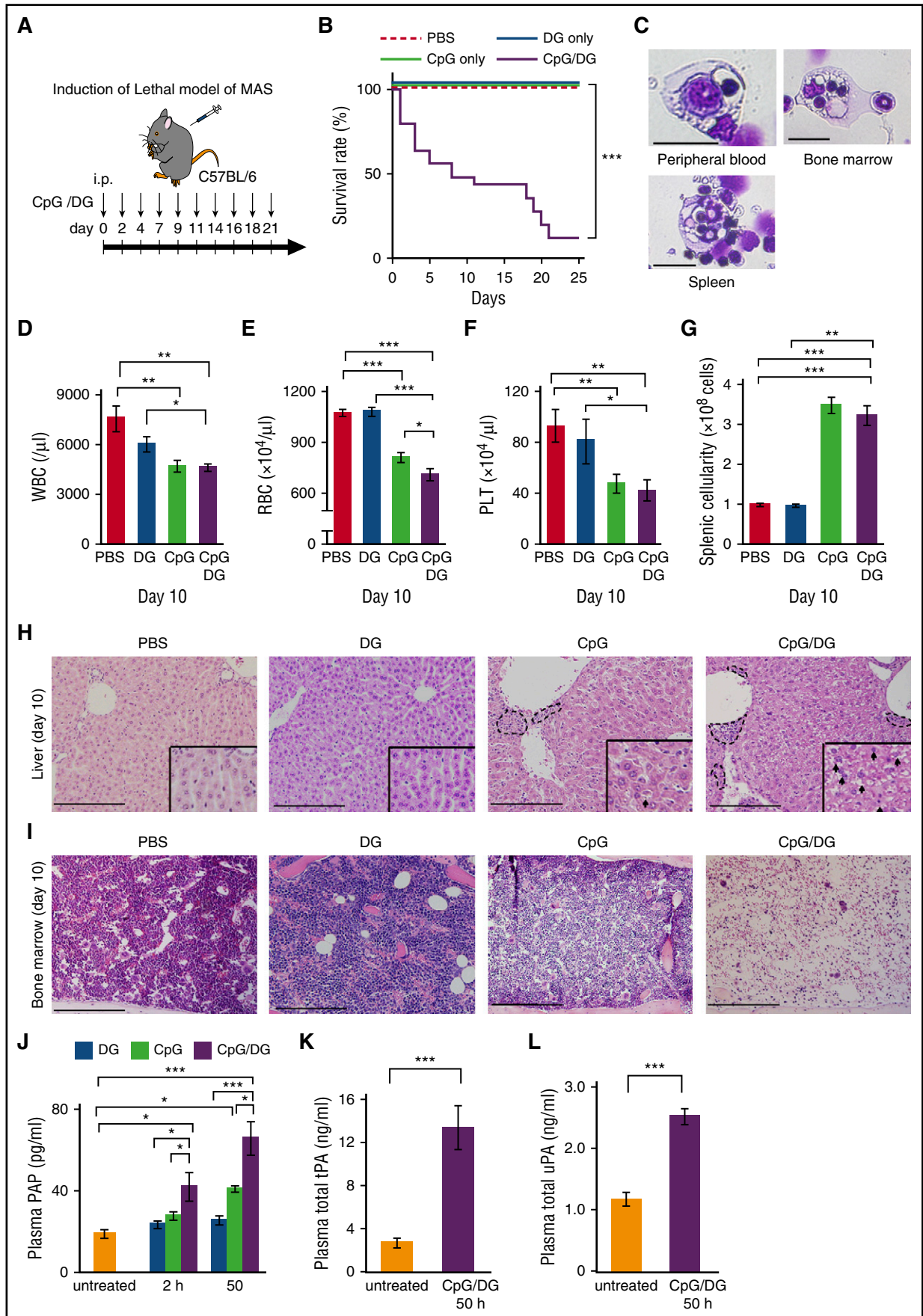


Figure 1.

(DG) enhances TLR-9 signaling in mice leading to TNF- $\alpha$ /TNFR1 activation and hepatocyte apoptosis.<sup>33</sup> Furthermore, DG-sensitized mice succumb to lethal toxic shock due to macrophage-derived TNF- $\alpha$  causing fulminant apoptosis of liver cells.<sup>34</sup> We established a lethal murine MAS by adding DG to the repeated CpG injections. We demonstrate that inhibition of plasmin prevented the progression of MAS, and ameliorated the disease by suppressing the influx of inflammatory cells and the production of inflammatory cytokines/chemokines.

## Materials and methods

### Mice

Eight-week-old female C57BL/6 mice were purchased from Japan SLC Inc. Eight-week-old female *Mmp9*<sup>+/+</sup>, *Mmp9*<sup>-/-</sup>, *Plg*<sup>+/+</sup>, and *Plg*<sup>-/-</sup> mice were each used after at least 10 backcrosses onto a C57BL/6 background. Animal studies were approved by the Animal Review Board of the Institute of Medical Science, University of Tokyo.

### Reagents

Trans-4-aminomethylcyclohexanecarbonyl-Tyr(O-Pic)-octylamide (YO-2) (provided by Kobe Gakuin University) was dissolved in 200  $\mu$ L of phosphate-buffered saline (PBS) at 375  $\mu$ g/mL. The following reagents were used: CpG (sequence: 5'-tccatgacgttctcagctt-3' [bases are phosphorothioate]) (Fasmac), D-(+)-galactosamine hydrochloride (WAKO), mouse plasmin (Innovative Research).

### Cell culture

RAW-264.7 cells were cultured in Dulbecco modified Eagle medium supplemented with 10%(vol/vol) fetal bovine serum and antibiotics. RAW-264.7 cells ( $1 \times 10^5$  cells per well) were stimulated with 1  $\mu$ M CpG and 0.43 IU/mL mouse plasmin. RAW-264.7 cells ( $1 \times 10^5$  cells per well) were stimulated with 1  $\mu$ M CpG 1 hour after preincubation of cells with 5  $\mu$ M YO-2 or PBS.

### Induction of MAS in mice

MAS was induced in 8-week-old female C57BL/6, *Mmp9*<sup>+/+</sup>, *Mmp9*<sup>-/-</sup>, *Plg*<sup>+/+</sup>, and *Plg*<sup>-/-</sup> mice by intraperitoneally injecting CpG1826 (2.5  $\mu$ g/g body weight [BW]) and DG (0.25 mg/g BW) at indicated time points.

### Drug administration in MAS mice

MAS model mice were intraperitoneally injected with 3.75  $\mu$ g/g BW of YO-2 or PBS daily from day 0 or day 4 to day 25. YO-2 or PBS injections were performed 3 hours before the injections of CpG/DG when mice were injected on the same day.

### Cytokine and protein analysis

Enzyme-linked immunosorbent assay (ELISA) kits were used to measure murine plasma samples for TNF- $\alpha$ , IFN- $\gamma$ , and CCL2 (Biolegend Inc), Fas-L and

total MMP-9 (R&D Systems), plasmin- $\alpha$ 2 antiplasmin complexes (PAPs) and fibrinogen degradation products (FDPs) (Cusabio Biotech Co), thrombin-antithrombin complex (TAT) (Abcam), total urokinase-type plasminogen activator (uPA) and total tissue-type plasminogen activator (tPA) (Innovative Research Inc), and ferritin (ALPCO Diagnostics). Plasma was assayed for triglyceride levels using the Quantification Colorimetric/Fluorometric kit (BioVision).

### Immunohistochemistry

Paraffin tissue sections were washed with PBS, serum blocked, and stained with the first antibody (Ab) overnight at 4°C, followed by second Ab staining and development with diaminobenzidine chromogen (brown color). First antibody: anti-MMP9 Ab (R&D Systems), CD11b (clone M1-70; BD Pharmingen), F4/80 (clone A3-1; AbD Serotec). Secondary antibody: N-Histofine<sup>R</sup> Simple Stain Mouse MAX-PO(G) and MAX-PO(Rat) (Nichirei Biosciences Inc).

### Flow cytometric analysis

Cells were stained with: CD11b-phycoerythrin (PE) Cy7, CD11c-PE, Ly6g-allophycocyanin (APC), Ly6c-PE, CD3e-APC, B220-PE (BD Pharmingen), F4/80-fluorescein isothiocyanate (FITC), TER119-Pacific Blue, APC Cy7-streptavidin (Biolegend), CD71-biotin (eBioscience), CCR2-FITC (R&D Systems). Cells were also stained with propidium iodide to exclude dead cells. Cells ( $5 \times 10^5$ ) were analyzed on a BD FACS Verse/Arial.

### Gelatin zymography

For more details, see Heissig et al.<sup>35</sup> Band densities were quantified using image analysis software (ImageJ).

### Western blotting

RAW cells were lysed with lysis buffer (Cell Signaling Technology) according to the manufacturer's instructions. For more details, see Sato et al.<sup>3</sup>

### Plasmin concentration assay

Samples were incubated with thrombin (1 U/mL) and fibrinogen (5 mg/mL) at 37°C for 30 minutes then put on ice for 2 minutes. Samples were centrifuged at 15 000 rpm for 5 minutes. Supernatants were recovered and the protein content, representing degradation products of fibrin in the presence of plasmin, was measured at 280 nm.

### Quantitative real-time PCR analysis

Total RNA was extracted using RNA TRIzol (Invitrogen), and complementary DNA (cDNA) was generated according to the manufacturer's protocols. This cDNA (10 ng) was used as a template for each polymerase chain reaction (PCR) amplification using the following specific forward and reverse primer pairs, respectively: mouse *I8s-rRNA* (5'-ccgaagcgttactcttgaaaaa-3') and (5'-tccattatcc tagctgcggtatc-3'); mouse *uPA* (5'-gtcctctctgcaacagagtc-3') and (5'-ctgtgtc tgagggtatgct-3'); mouse *uPAR* (5'-tctggtatctcagagcttc-3') and (5'-agcacatc taagcctgtagc-3'); mouse *MMP9* (5'-ggtaactggaagatgctgtg-3') and (5'-tg aagtctcagaaggtggat-3'); mouse *TNF- $\alpha$*  (5'-gccgattgctatcctacac-3') and (5'-gggtataggctcaccag-3'); mouse *CCL2* (5'-tcctgtcatgctctgg-3') and (5'-ctgctgtgctatcctctgta-3'). For quantitative real-time PCR, PCR mixtures

**Figure 1. Fulminant MAS in mice after injection with TLR9 agonist, CpG, and DG leads to the activation of plasminogen/plasmin.** (A) CpG and DG were administered intraperitoneally into 8-week-old female C57BL/6 mice at days 0, 2, 4, 7, 9, 11, 14, 16, 18, and 21 (0h, 48h, 96h, 168h, ...). (B) Survival rate of PBS- (n = 10), DG- (n = 10), CpG- (n = 10), or CpG/DG-injected mice (n = 25). (C) Wright-Giemsa-stained slides of peripheral blood, BM, and spleen cells of CpG/DG-injected mice at day 10 show engulfment of erythrocytes in macrophages, so-called hemophagocytosis. Bar represents 20  $\mu$ m. (D-F) (D) Counts of white blood cells (WBC), (E) red blood cells (RBC), and (F) platelets (Plt) of PBS-, DG-, CpG-, or CpG/DG-injected mice at day 10 (n = 5-7 per group). (G) Number of mononuclear cells in spleens of PBS-, DG-, CpG-, or CpG/DG-injected mice at day 10 (n = 5-7 per group). (H) Representative images of hematoxylin-and-eosin (H&E)-stained sections of the liver from PBS-, DG-, CpG-, or CpG/DG-injected mice at day 10. Bars represent 200  $\mu$ m. Black dotted lines indicate mononuclear cell infiltration; black arrows, hepatocellular degeneration. (I) Representative images of H&E-stained sections of the BM from PBS-, DG-, CpG-, or CpG/DG-injected mice at day 10. Bars represent 200  $\mu$ m. (J) Plasma PAP levels of untreated mice, DG-, CpG-, or CpG/DG-injected mice at 2 hours and 50 hours (n = 5-7 per group). (K) Plasma levels of total tPA of untreated mice and CpG/DG-injected mice 50 hours after CpG/DG injection (n = 5-6 per group). (L) Plasma levels of total uPA of untreated mice and CpG/DG-injected mice 50 hours after CpG/DG injection (n = 5-6 per group). Data represent mean  $\pm$  SEM. \**P* < .05, \*\**P* < .01, \*\*\**P* < .001, using 1-way ANOVA with the Tukey posttest or the unpaired, 2-tailed Student *t* test for significance and using the log-rank test for survival curves.

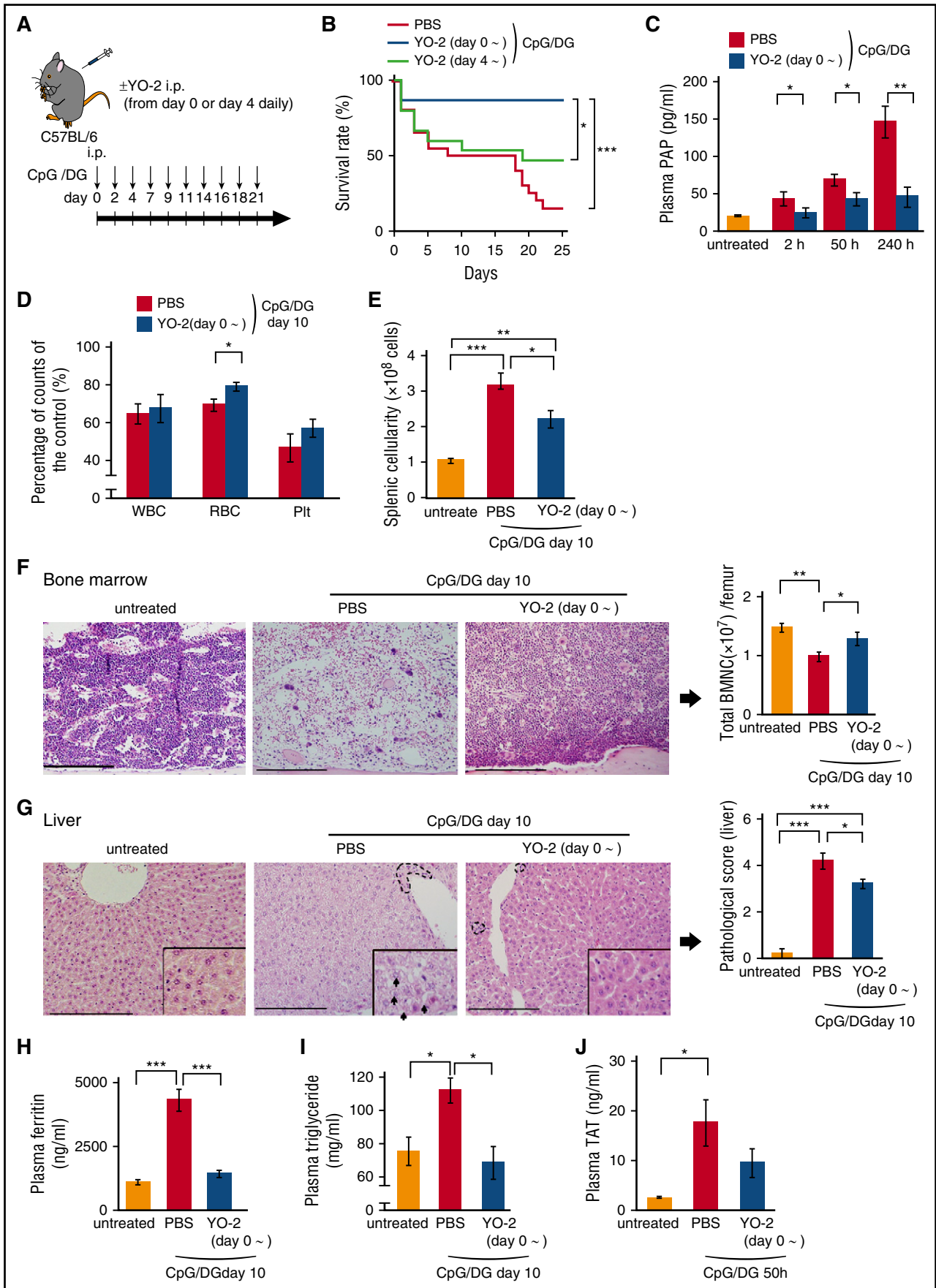


Figure 2.



were prepared using SYBR Premix Ex TaqII (Takara) containing 0.2 mM of each primer, and amplification reactions were performed. Gene expression levels were measured using the ABI Prism 7500 sequence detection system (Applied Biosystems). PCR product levels were estimated by measurement of the intensity of SYBR Green fluorescence.

### Statistical analysis

All data are presented as means  $\pm$  standard error of the mean (SEM). All *P* values were calculated by 1-way analysis of variance (ANOVA) with the Tukey posttest or the Student unpaired 2-tailed *t* test, as appropriate. Survival curves were plotted using Kaplan-Meier estimates with the log-rank test. *P* < .05 was considered statistically significant.

## Results

### Repeated injections of the TLR-9 agonist and DG cause fulminant MAS in mice and lead to the activation of plasminogen/plasmin

The recently published murine model of MAS using TLR-9 agonist CpG injections does not induce lethality.<sup>32</sup> Coinjection of DG with CpG,<sup>33,34</sup> but neither CpG nor DG alone, caused high lethality in C57BL/6 mice (Figure 1A-B). Cytospins of splenocytes, peripheral blood, and bone marrow (BM) cells derived from CpG/DG-injected mice at day 10 showed erythrocyte engulfment by macrophages, a typical sign of hemophagocytosis (Figure 1C). In addition, CpG/DG-injected mice showed characteristic features of MAS including peripheral pancytopenia associated with a hypocellular BM, splenomegaly, and liver damage with mononuclear cell infiltration (Figure 1D-I). The addition of DG to CpG, but not DG alone, increased circulating plasmin levels in vivo (Figure 1J). We chose this murine MAS model for further analysis because it fulfilled 5 of 8 criteria required to diagnose HLH/HPS in humans (supplemental Table 1, see supplemental Data available at the *Blood* Web site). Deaths were observed in CpG/DG-injected mice (Figure 1B). Early-phase deaths coincided with the development of severe liver damage whereas later deaths coincided with severe BM suppression (Figure 1H-I).

Plasma levels of PAP levels were higher in CpG/DG-injected mice compared with CpG-injected mice (Figure 1J). Plasma levels of uPA and tPA were elevated after CpG/DG injection (Figure 1K-L), indicating that the fibrinolytic system was accelerated in fulminant MAS.

### Plasminogen/plasmin deficiency ameliorates MAS disease progression in mice

To understand the role of plasmin during the progression of fulminant MAS, the treatment of plasmin inhibitor YO-2 was started from either

day 0 or day 4 (Figure 2A). YO-2 blocks the catalytic site of plasmin and efficiently inhibits circulating plasmin.<sup>36</sup> When YO-2 injection was delayed starting from day 4, the early death occurring within the first week could not be prevented. In contrast, daily injections of YO-2 starting from day 0 protected mice from early and delayed death (Figure 2B), indicating that plasmin was responsible for early and late death. YO-2 was given starting from day 0 in further experiments. YO-2 prevented the time-dependent upregulation of plasma PAP (Figure 2C).

Although leukopenia and thrombocytopenia persisted, YO-2-treated mice showed a lower degree of anemia (Figure 2D) and reduced MAS-associated spleen enlargement (Figure 2E). YO-2 treatment prevented hematopoietic cell depletion within the BM at day 10 (Figure 2F). Histopathological analysis of the liver revealed a reduction of infiltrating mononuclear cells and less tissue damage at day 10 in YO-2-treated mice (Figure 2G). CpG/DG-injected, but not YO-2-treated mice developed hyperferritinemia and hypertriglyceridemia, as described in patients with MAS (Figure 2H-I).

Although fibrinogen plasma level elevation occurred independent of plasmin inhibition (supplemental Figure 1A), the generation of FDPs, as a measure of increased fibrinolysis, was inhibited in YO-2-treated mice at day 10 (supplemental Figure 1B), indicating that YO-2 blocked fibrinolysis. Elevated plasma levels of TAT in CpG/DG-injected mice were detected, but significant differences in plasma TAT levels were not observed between PBS- and YO-2-treated mice (Figure 2J). These data suggest that although the coagulation system is activated during MAS progression, YO-2 did not exaggerate coagulation while suppressing fibrinolysis.

Liver apoptosis has been reported in DG-sensitized mice treated with CpG.<sup>33</sup> Liver sections from YO-2-treated MAS mice showed less TUNEL<sup>+</sup> YO-2 cells (supplemental Figure 1C). These findings demonstrate that plasmin can control the induction of hepatocyte apoptosis after CpG/DG injection. To examine the role of plasmin on erythropoiesis in YO-2-treated animals, erythroblast numbers (Ter119<sup>+</sup>CD71<sup>+</sup> cells) were quantified (supplemental Figure 1D-G). MAS mice showed reduced numbers of BM erythroblasts whereas the splenic erythroblast number increased (supplemental Figure 1D-E), a trend inhibited by YO-2 treatment. Apoptotic cells are Annexin V<sup>+</sup> and propidium iodide negative. A 10-fold increase in the percentage of Annexin V<sup>+</sup> erythroblasts within the spleen of untreated MAS compared with PBS-treated mice was found. Fewer Annexin V<sup>+</sup> erythroblasts were found in splenocytes of YO-2-treated mice (supplemental Figure 1F-G), suggesting that plasmin can influence splenic erythroblast apoptosis during MAS development.

*Plg*<sup>-/-</sup> mice suffer a progressive wasting disease and develop other spontaneous pathologies.<sup>37</sup> To understand the role of plasminogen/plasmin activation during MAS progression, we examined plasminogen-deficient (*Plg*<sup>-/-</sup>) mice. CpG/DG-injected *Plg*<sup>-/-</sup> mice

**Figure 2. Plasmin inhibitor treatment prevents MAS-associated lethality and tissue destruction.** (A) Experimental schedule for the induction of MAS using CpG/DG intraperitoneal injections, and cotreatment with the plasmin inhibitor YO-2 starting from day 0 or from day 4. (B) Survival rate of CpG/DG-injected mice treated with PBS (n = 20) or YO-2 with treatment starting on day 0 (day 0~; n = 15) or day 4 (day 4~; n = 15). (C) PAP levels were determined at indicated time points in plasma samples of control and CpG/DG-injected mice coinjected with PBS or YO-2 (n = 5-10 per group). (D) Percentage of WBC, RBC, and Plt in CpG/DG-injected mice treated with PBS or YO-2 (day 0~) at day 10 (n = 10 per group) (set as 100% for day 0). (E) Spleen cell counts at day 10 of untreated and CpG/DG-injected mice administered with PBS or YO-2 (day 0~) (n = 7 per group). (F) Representative images of H&E-stained BM sections of untreated and CpG/DG-injected mice treated with PBS or YO-2 (day 0~) at day 10. Scale bars = 200  $\mu$ m. Right panel, Total number of BM nucleated cells per femur (n = 5 per group). (G) Representative images of H&E-stained liver sections from untreated and CpG/DG-injected mice treated with PBS/carrier or YO-2 (day 0~) at day 10. Scale bars = 200  $\mu$ m. Black dotted lines indicate mononuclear cell infiltration; black arrows, hepatocellular degeneration. Right panel, Histopathological liver score in groups of these mice (n = 5 per group). Cell infiltration: none = 0, mild = 1, moderate = 2, severe = 3. Liver damage: none = 0, mild = 1, moderate = 2, severe = 3. (H) Plasma ferritin levels of untreated mice and CpG/DG-injected mice injected with PBS or YO-2 at day 10 (n = 5 per group). (I) Plasma triglyceride levels of untreated mice and CpG/DG-injected mice treated with PBS or YO-2 at day 10 (n = 5 per group). (J) Plasma TAT levels of untreated mice and CpG/DG-injected mice treated with PBS or YO-2 50 hours after CpG/DG injection (n = 5 per group). Data represent mean  $\pm$  SEM. \**P* < .05, \*\**P* < .01, \*\*\**P* < .001, using 1-way ANOVA with the Tukey posttest or the unpaired, 2-tailed Student *t* test for significance and using the log-rank test for survival curves. BMNC, bone marrow nucleated cells; i.p., intraperitoneally.

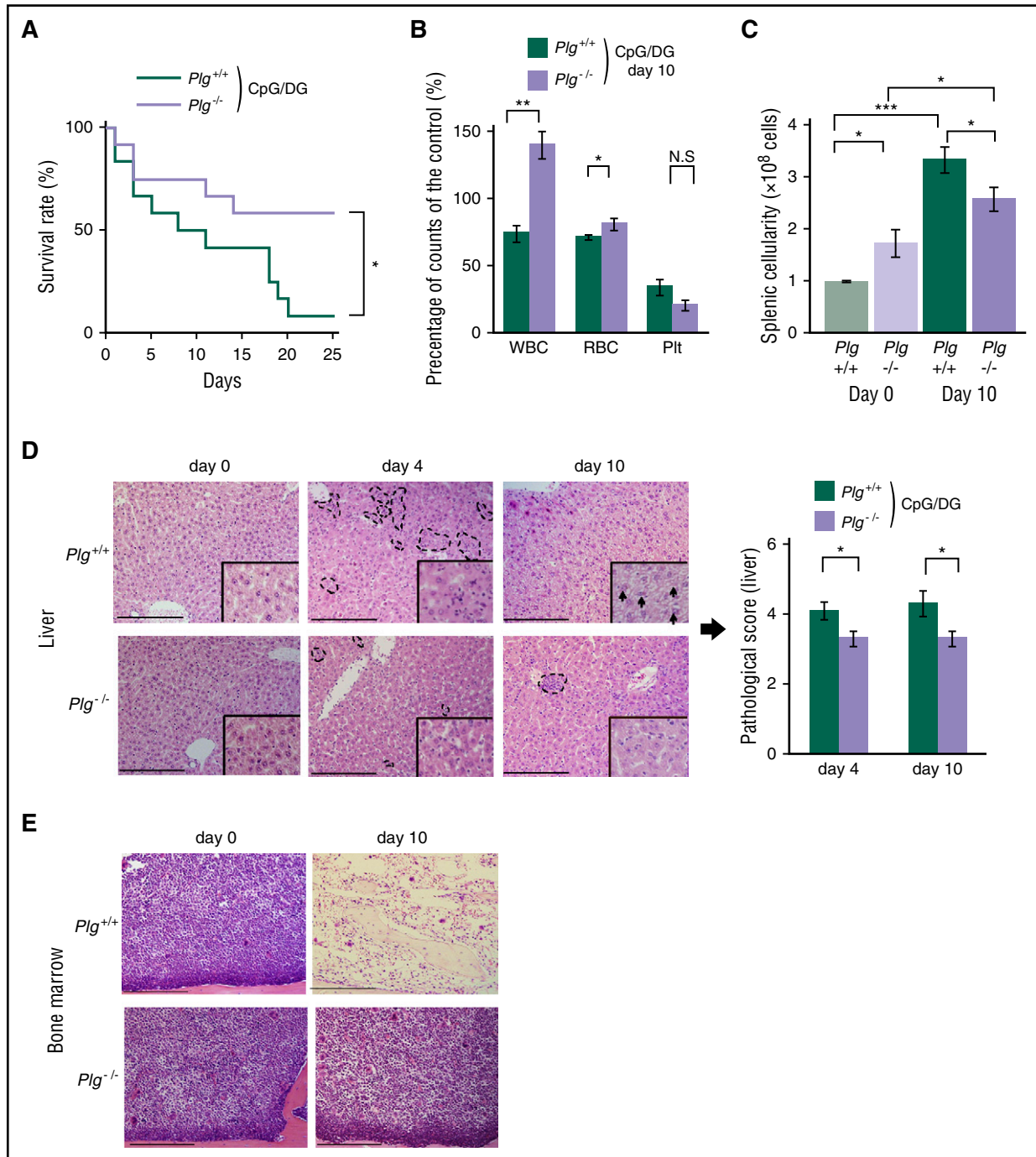


**Figure 3. Plasminogen deficiency suppresses clinical symptoms of MAS in CpG/DG-injected mice.** (A) Survival rate of CpG/DG-injected  $Plg^{+/+}$  or  $Plg^{-/-}$  mice ( $n = 12$  per group). (B) Percentage of WBC, RBC, and PLT set as 100% for day 0 in CpG/DG-injected  $Plg^{+/+}$  or  $Plg^{-/-}$  mice at day 10 ( $n = 6-8$  per group). (C) Mononuclear spleen cell counts of CpG/DG-injected  $Plg^{+/+}$  or  $Plg^{-/-}$  mice at day 0 and day 10 ( $n = 5-7$  per group). (D) Representative images of H&E-stained sections of liver isolated from CpG/DG-injected  $Plg^{+/+}$  or  $Plg^{-/-}$  mice at days 0, 4, and 10. Scale bars = 200  $\mu$ m. Black dotted lines indicate mononuclear cell infiltration; black arrows, hepatocellular degeneration. Right panel, Histopathological liver score in groups of these mice ( $n = 5$  per group). (E) Representative H&E-stained BM section images of CpG/DG-injected  $Plg^{+/+}$  or  $Plg^{-/-}$  mice at day 0 and day 10. Scale bars = 200  $\mu$ m. Data represent mean  $\pm$  SEM. \* $P < .05$ , \*\* $P < .01$ , \*\*\* $P < .001$ , using 1-way ANOVA with the Tukey posttest or the unpaired, 2-tailed Student  $t$  test for significance and using the log-rank test for survival curves. N.S., not significant.

revealed a lower mortality rate than  $Plg^{+/+}$  mice (Figure 3A) lacking protection from early, but not late, death. Anemia was less severe in  $Plg^{-/-}$  mice (Figure 3B; supplemental Figure 2A-C). Splenic cellularity was increased at baseline in  $Plg^{-/-}$  mice.<sup>38</sup> MAS-associated splenomegaly was less pronounced in  $Plg^{-/-}$  than in  $Plg^{+/+}$  mice (Figure 3C). Reduced numbers of infiltrating

mononuclear cells and less tissue damage indicated a low pathological score in  $Plg^{-/-}$  liver tissues at day 4 and day 10 (Figure 3D), and a decreased BM cellularity was observed in  $Plg^{-/-}$  BM sections at day 10 (Figure 3E). These data indicate that genetic plasminogen deficiency prevented clinical symptoms of murine MAS.

### MMP-9 inhibition suppresses MAS progression in mice

Plasmin can activate MMPs like MMP-9 either directly or indirectly.<sup>39</sup> MMP-9 activation contributes to tissue damage during inflammation.<sup>3,4,19</sup> To understand the mechanism of how plasmin inhibition can prevent MAS progression, we focused on the role of MMP-9. Elevated plasma levels of total MMP-9, both pro and active forms, but not MMP-2, were found in CpG/DG-injected mice (Figure 4A). Increased levels of circulating MMP-9 were detected in MAS controls but not YO-2-treated mice (Figure 4B). Similarly, fewer MMP-9<sup>+</sup> liver cells were found in CpG/DG-injected YO-2-treated mice (Figure 4C).

To understand the functional significance of MMP-9 for the progression of MAS, we used MMP-9 gene-deficient mice (*Mmp9*<sup>-/-</sup> mice). Compared with *Mmp9*<sup>+/+</sup> mice, MAS-induced *Mmp9*<sup>-/-</sup> showed an improved survival rate, and amelioration of other MAS-related clinical features, such as anemia, splenomegaly (Figure 4D-F), infiltrating mononuclear cells in liver tissues at day 4 and tissue damage at day 10 (Figure 4G), and hypocellular BM (Figure 4H). These data suggest that plasmin and MMP-9 are activated during MAS progression, and that MMP-9 seems to be a downstream target of plasmin during MAS progression in vivo.

To examine whether the beneficial effect of YO-2 is driven by its potential to prevent the activation of plasminogen/plasmin and MMP-9, we treated *Plg*<sup>-/-</sup> and *Mmp9*<sup>-/-</sup> mice with YO-2. Additional treatment with YO-2 did not further increase the survival rate in *Plg*<sup>-/-</sup> or *Mmp9*<sup>-/-</sup> mice (supplemental Figure 3A-B), indicating that the effect of YO-2 on the clinical improvement in MAS symptoms was due to its potential to inhibit the activation of plasminogen/plasmin and MMP-9.

### Plasmin inhibition attenuates the production of inflammatory cytokines/chemokines in MAS model mice

Central to the pathogenesis of MAS is a cytokine storm, with markedly increased levels of numerous proinflammatory cytokines including IL-1, IL-6, TNF- $\alpha$ , and IFN- $\gamma$ .<sup>1,2</sup> Previous studies showed that plasmin binds to monocytes/macrophages, and can alter the expression of cytokines such as TNF- $\alpha$ , IL-1, IL-6, and CCL2.<sup>13,16,40</sup> CCL2 can recruit monocytes, T cells, and dendritic cells to sites of inflammation. Plasma TNF- $\alpha$  levels were increased in CpG- or CpG/DG-injected mice (data not shown). Plasmin deficiency, induced by YO2 treatment or by genetic depletion using *Plg*<sup>-/-</sup> mice, and MMP-9 deficiency attenuated TNF- $\alpha$  increases (Figure 5A-C). Similarly, YO-2 diminished plasma Fas-L and CCL2 (Figure 5D-E) but not IFN- $\gamma$  levels (Figure 5F). These data indicate that the blockade of plasmin during MAS progression reduced the production of inflammatory cytokines/chemokines.

### Plasmin inhibition reduces the number of infiltrating monocytes/macrophages in the target organs in MAS model mice

Patients with juvenile idiopathic arthritis had higher plasma levels of TNF- $\alpha$  and CCL2.<sup>41</sup> Plasmin enhances CCL2-CCR2 signaling by releasing a CCL2 fragment with improved chemoattractive ability.<sup>3,42</sup> Given that YO-2 reduced plasma CCL2 levels (see Figure 5E), and CCL2, after binding to its receptor CCR2, induces monocyte recruitment,<sup>20</sup> we examined the role of plasmin for the recruitment of inflammatory cells. YO-2 reduced the number of splenic CCR2<sup>+</sup>, CD11b<sup>+</sup>, and CD3<sup>+</sup>, but not B220<sup>+</sup> cells (Figure 6A-B). A detailed analysis of the CD11b<sup>+</sup> cell population revealed that YO-2 reduced the number of myeloid dendritic CD11b<sup>+</sup>CD11c<sup>+</sup> cells, CD11b<sup>+</sup>F4/80<sup>+</sup> macrophages, and CD11b<sup>+</sup>Ly6g<sup>low</sup>Ly6c<sup>high</sup> inflammatory monocytes in splenocytes (Figure 6C). YO-2 prevented the influx of CD11b<sup>+</sup> cells in the liver (Figure 6D), and F4/80<sup>+</sup> cells in the BM and the liver (Figure 6D-E), indicating that plasmin inhibition suppressed the

infiltration of monocytes/macrophages into the major target organs in MAS.

### tPA administration worsens clinical symptoms of MAS and shortens survival in MAS-induced mice

During the progression of MAS, increased tPA levels were detectable (see also Figure 1K). tPA can modulate the inflammatory response to tissue injury in various models.<sup>43</sup> tPA treatment shortened survival in MAS mice (supplemental Figure 4A) and worsened clinical symptoms such as severe leukopenia, thrombocytopenia, and splenomegaly with augmented numbers of infiltrating mononuclear cells into liver tissues at day 4 (supplemental Figure 4C-F). As early as 1 hour after tPA coinjection with CpG/DG, MAS mice showed a significant elevation in plasma TNF- $\alpha$  levels when compared with non-tPA-treated MAS mice (supplemental Figure 4G), suggesting that tPA accelerates inflammation during MAS progression.

### Plasmin potentiates CpG-mediated TLR-9 signaling on macrophages

TLR-9 recognizes CpG in endosomes leading to macrophage activation.<sup>44</sup> It was demonstrated that plasmin potentiates TLR-4 signaling.<sup>45</sup> The addition of the TLR-9 agonist CpG increased the gene expression of uPA, uPA receptor (uPAR), and MMP-9 in cultured RAW264.7 cells (Figure 7A). YO-2 addition inhibited plasmin generation and TNF- $\alpha$  production induced by CpG (Figure 7B-C), indicating that plasmin might enhance TLR-9 signaling.

TLRs signal through the recruitment of specific adaptor molecules, leading to the activation of the transcription factors NF- $\kappa$ B.<sup>46</sup> The addition of plasmin and CpG additively enhanced the expression of TNF- $\alpha$ , CCL2, and MMP-9 and activated the NF- $\kappa$ B signaling pathway (Figure 7D-G). These data provide evidence that plasmin, by enhancing TLR-9 signaling and NF- $\kappa$ B signaling, augments monocyte cytokines/chemokine expression that contributes to the inflammatory response.

## Discussion

In the present study, we provide genetic and functional evidence that the activation of plasminogen/plasmin and MMP-9 during experimental fulminant MAS contributes systemic inflammation, a process in part mediated by the increase in monocytes/macrophages in the target tissues and the release of inflammatory cytokines/chemokines. Pharmacological inhibition of plasmin reduced tissue damage and prevented inflammation-associated lethality in a murine fulminant MAS model. Our data introduce a novel paradigm by which plasmin mediates systemic inflammatory responses, and provide evidence for essential roles of the fibrinolytic system during the progression of MAS.

### A fulminant MAS model

Although many of the clinical MAS symptoms observed in humans can be recapitulated by TLR-9 activation in mice, no lethality was observed in CpG-injected mice.<sup>32,47</sup> But in some familial HLH/HPS patients, multiple organ dysfunction occurs leading to the death. With the knowledge that TLR-9 stimulation induces a fulminant liver pathology in DG-sensitized mice by enhancing the sensitivity to TNF- $\alpha$ ,<sup>33,34</sup> we included DG to the CpG injection schedule. TNF- $\alpha$  levels between CpG- or CpG/DG-treated mice were not significantly different (data not shown), implying that other factors might be responsible for the severe

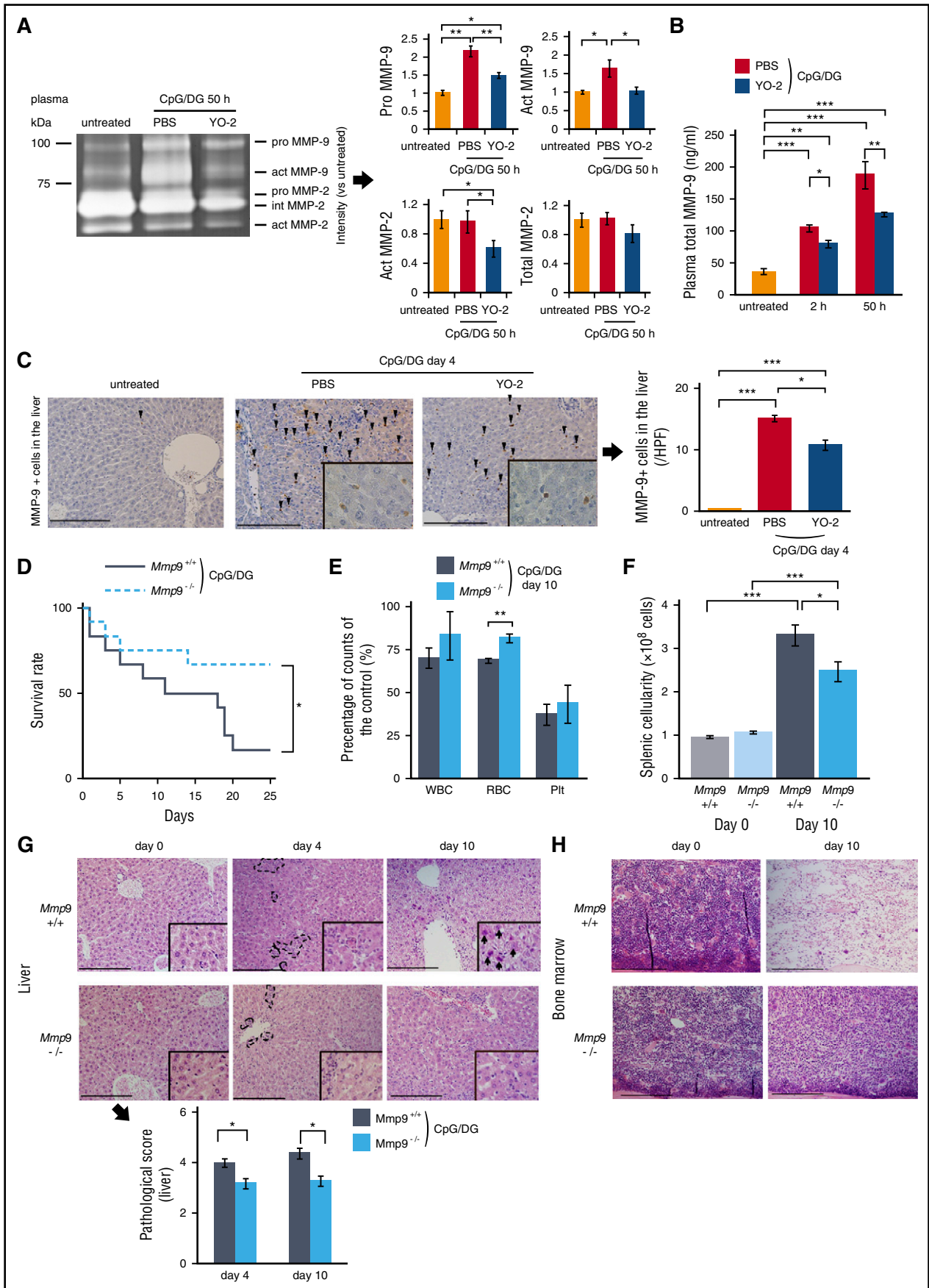
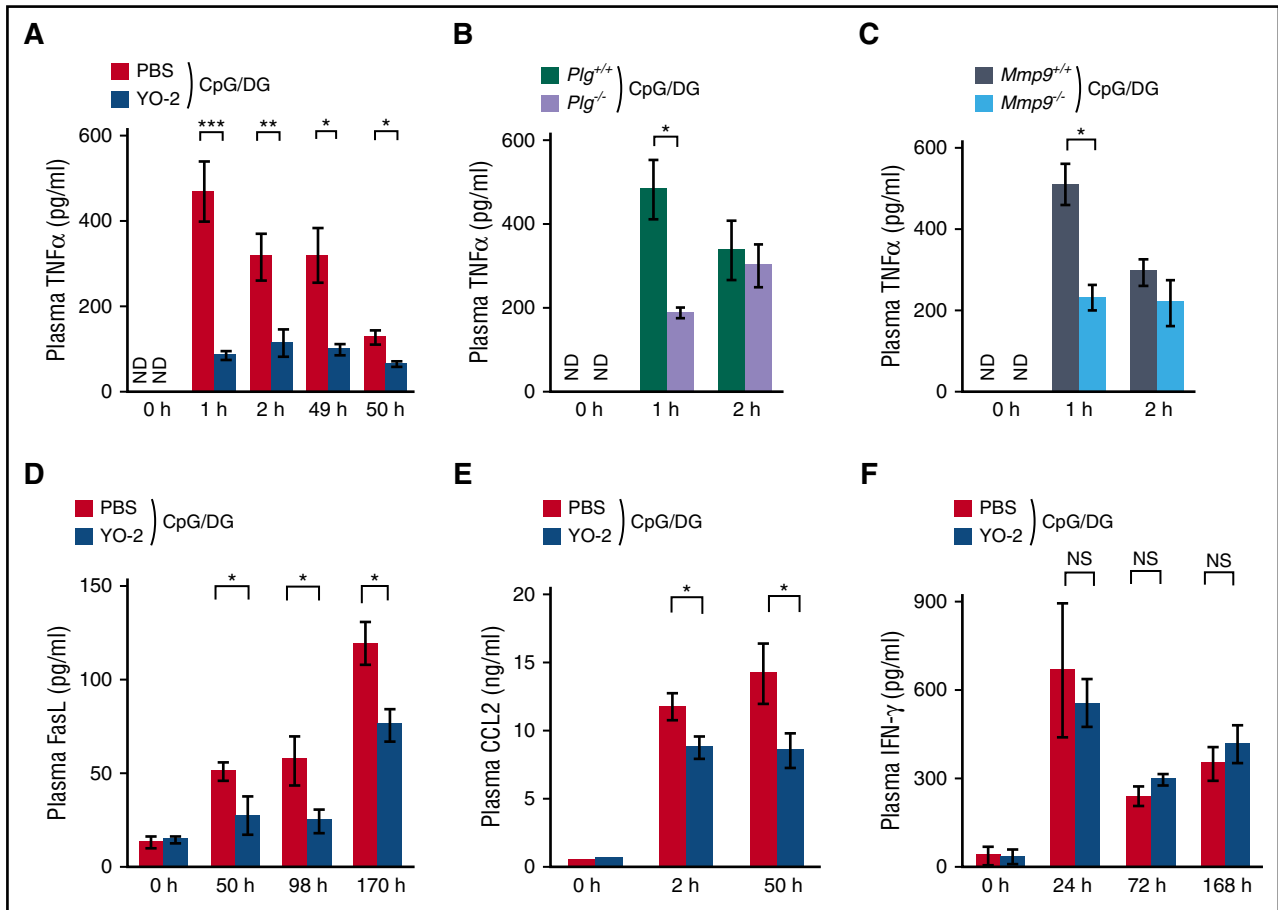


Figure 4.





**Figure 5. Plasmin and MMP-9 inhibition reduces the production of several inflammatory cytokines/chemokines in MAS mice.** (A-C) Plasma TNF- $\alpha$  levels were determined at indicated time points in samples from CpG/DG-injected (A), *Plg*<sup>+/+</sup> and *Plg*<sup>-/-</sup> (B), and *Mmp9*<sup>+/+</sup> and *Mmp9*<sup>-/-</sup> (C) mice treated with PBS or YO-2 (n = 3-6 per group). (D-F) Plasma Fas-L (D), CCL2 (E), and IFN- $\gamma$  (F) levels were determined at indicated time points in samples from CpG/DG-injected mice treated with PBS or YO-2 (n = 3-6 per group). Data represent mean  $\pm$  SEM. \**P* < .05, \*\**P* < .01, \*\*\**P* < .001, using 1-way ANOVA with the Tukey posttest or the unpaired, 2-tailed Student *t* test for significance. ND, not detected.

clinical progression. Early studies reported that DG-treated rats showed an increased catabolism for fibrinogen.<sup>48</sup>

Signaling through other death receptors, for example, Fas/Fas-L might be responsible for the fulminant phenotype observed. Plasmin can cleave Fas-L releasing a soluble proapoptotic Fas-L fragment from, for example, endothelial cells.<sup>49</sup> Further studies will be necessary to determine the role of Fas-L in the MAS model. We showed DG addition to CpG strongly induced plasminogen/plasmin activation in vivo. The plasmin inhibitor YO-2 controlled the lethality better in CpG/DG-induced MAS but not in CpG-induced MAS mice (data not shown).

Plasmin/plasminogen deficiency prevented the late, but not the early, death after CpG/DG injections in MAS mice. Early death in our established MAS model seems to be dependent on a massive induction of apoptosis of liver cells as early as day 4 that is driven by plasmin.

These data are in concordance with earlier studies demonstrating that plasminogen deficiency leads to impaired remodeling after toxic liver injury.<sup>50</sup> In these earlier studies, it was demonstrated that *Plg*<sup>-/-</sup>/*fibrinogen*<sup>-/-</sup> mice did not correct the abnormal phenotype, and they concluded that plasminogen deficiency impedes the clearance of necrotic tissue from a diseased hepatic microenvironment and the subsequent reconstitution of normal liver architecture in a fashion that is unrelated to circulating fibrinogen.

MMP-9 and plasminogen deficiency prevented the late onset of death and reduced circulating plasma TNF- $\alpha$  levels. But the role of TNF- $\alpha$  for the pathogenesis of MAS is not so clear. We suggest that MMP-9 and plasminogen deficiency reduces tissue damage in part by preventing extracellular matrix degradation and cytokine activation. But further studies will be necessary to address this in more detail.

**Figure 4. Plasmin drives MMP-9 upregulation worsens clinical outcome in CpG/DG-injected MAS mice.** (A) Blood samples retrieved 50 hours after CpG/DG injection from control and CpG/DG-injected mice treated with PBS or YO-2 were analyzed by gelatin zymography. Right panels, The quantification of the intensity of pro MMP-9, active MMP-9, active MMP-2, and total MMP-2 bands were analyzed by comparing to the bands of untreated mice (n = 3 per group). (B) Total plasma MMP-9 levels of untreated mice and CpG/DG-injected mice treated with PBS or with YO-2 at indicated time points (n = 5-7 per group). (C) Representative images of MMP-9 immunostained liver sections derived from untreated mice and CpG/DG-injected mice treated with PBS or YO-2 at day 4. Scale bars = 200  $\mu$ m. Black arrows indicate MMP-9<sup>+</sup> cells. Right panel, The quantification of MMP-9<sup>+</sup> cells in liver sections from untreated and CpG/DG-injected mice treated with PBS or YO-2 at day 4 (n = 5 per group). (D) Survival rate of CpG/DG-injected *Mmp9*<sup>+/+</sup> or *Mmp9*<sup>-/-</sup> mice (n = 12 per group). (E) Percentage of blood counts of CpG/DG-injected *Mmp9*<sup>+/+</sup> or *Mmp9*<sup>-/-</sup> mice at day 10 (set as 100% for day 0). (F) Spleen cell number from CpG/DG-injected *Mmp9*<sup>+/+</sup> or *Mmp9*<sup>-/-</sup> mice at day 0 and 10 (n = 5 per group). (G) Representative images of H&E-stained liver sections of CpG/DG-injected *Mmp9*<sup>+/+</sup> or *Mmp9*<sup>-/-</sup> mice at day 0, 4, and 10. Scale bars = 200  $\mu$ m. Black dotted lines indicate mononuclear cell infiltration; blue arrows, hepatocellular degeneration. Bottom panel, histopathological scores of CpG/DG-injected *Mmp9*<sup>+/+</sup> or *Mmp9*<sup>-/-</sup> mice at day 4 and 10 (n = 5 per group). (H) Representative images of H&E-stained BM sections of CpG/DG-injected *Mmp9*<sup>+/+</sup> or *Mmp9*<sup>-/-</sup> mice at day 0 and day 10. Bars represent 200  $\mu$ m. Data represent mean  $\pm$  SEM. \**P* < .05, \*\**P* < .01, \*\*\**P* < .001, using 1-way ANOVA with the Tukey posttest or the unpaired, 2-tailed Student *t* test for significance and using the log-rank test for survival curves. HPF, high-powered field.

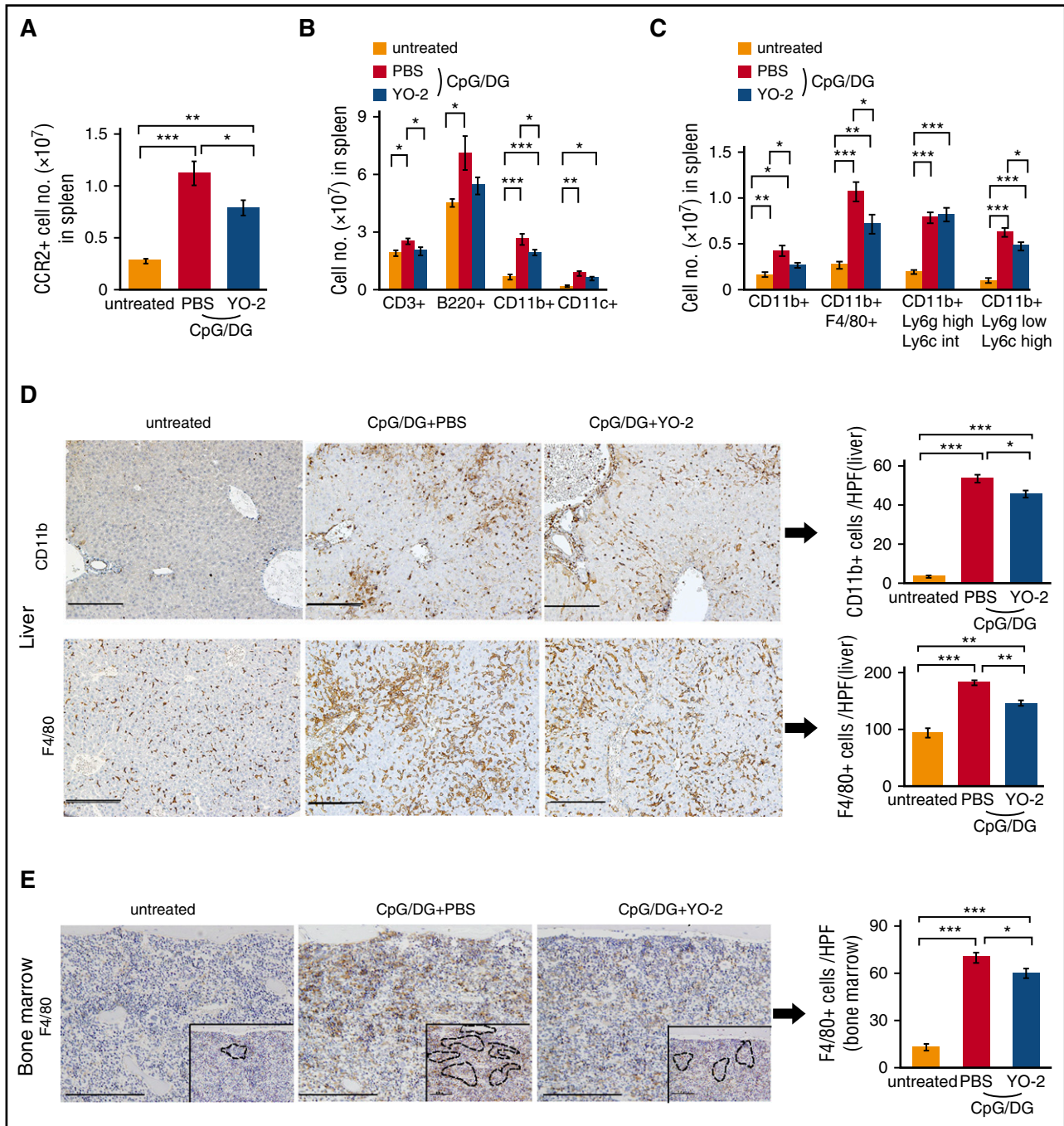


**Figure 6. YO-2 treatment suppresses the infiltration of inflammatory cells into spleen, liver, and BM of CpG/DG-injected mice.** (A) Absolute numbers of CCR2<sup>+</sup> cells in spleen derived from untreated and CpG/DG-injected mice after treatment with PBS or YO-2 at day 7 (n = 5-7 per group). (B) Absolute numbers of CD3<sup>+</sup>, B220<sup>+</sup>, CD11b<sup>+</sup>, and CD11c<sup>+</sup> cells in spleens of untreated and CpG/DG-injected mice following treatment with PBS or YO-2 as determined at day 7 (n = 5-7 per group). (C) Absolute numbers of these 4 fractions of CD11b<sup>+</sup> cells in the spleen of untreated mice and CpG/DG-injected mice treated with PBS or YO-2 at day 7 (n = 5-7 per group). (1) CD11b<sup>+</sup>CD11c<sup>+</sup> (myeloid dendritic cell), (2) CD11b<sup>+</sup>F4/80<sup>+</sup> (macrophage), (3) CD11b<sup>+</sup>Ly6g<sup>high</sup>Ly6c<sup>int</sup> (neutrophil), (4) CD11b<sup>+</sup>Ly6g<sup>low</sup>Ly6c<sup>high</sup> (inflammatory monocyte). (D) Representative images of the immunostaining of CD11b and F4/80 of liver sections derived from untreated and CpG/DG-injected mice treated with PBS or YO-2 at day 4 (left panels; bars represent 200  $\mu$ m). Right panel, the quantification of indicated positive cells per HPF in different treatment groups (n = 5 per group). (E) Representative images of the immunostaining of F4/80 of BM sections of untreated mice and CpG/DG-injected mice treated with PBS or YO-2 at day 4. Scale bars = 200  $\mu$ m. Black lines indicate F4/80<sup>+</sup> cells. Right panel, The quantification of F4/80<sup>+</sup> cells per HPF of tissue sections (n = 5 per group). Data represent mean  $\pm$  SEM. \**P* < .05, \*\**P* < .01, \*\*\**P* < .001, using 1-way ANOVA with the Tukey posttest or the unpaired, 2-tailed Student *t* test for significance.

Plg<sup>-/-</sup> mice are predisposed to severe thrombosis and develop spontaneous thrombotic lesions in visceral organs due to widespread multiorgan fibrin deposition.<sup>51</sup> The increased fibrinogen levels, the increased splenic cellularity, and the leukocytosis at the start of the study indicate that Plg<sup>-/-</sup> mice used in our study already showed phenotypic

symptoms of an elevated inflammation status. Although it is unclear at this point how fibrin affects MAS progression and further studies will be required to establish its role during MAS, studies in various inflammation models indicate that fibrin extravasation induces local inflammation. It is possible that fibrin accumulation during the early phase of the MAS

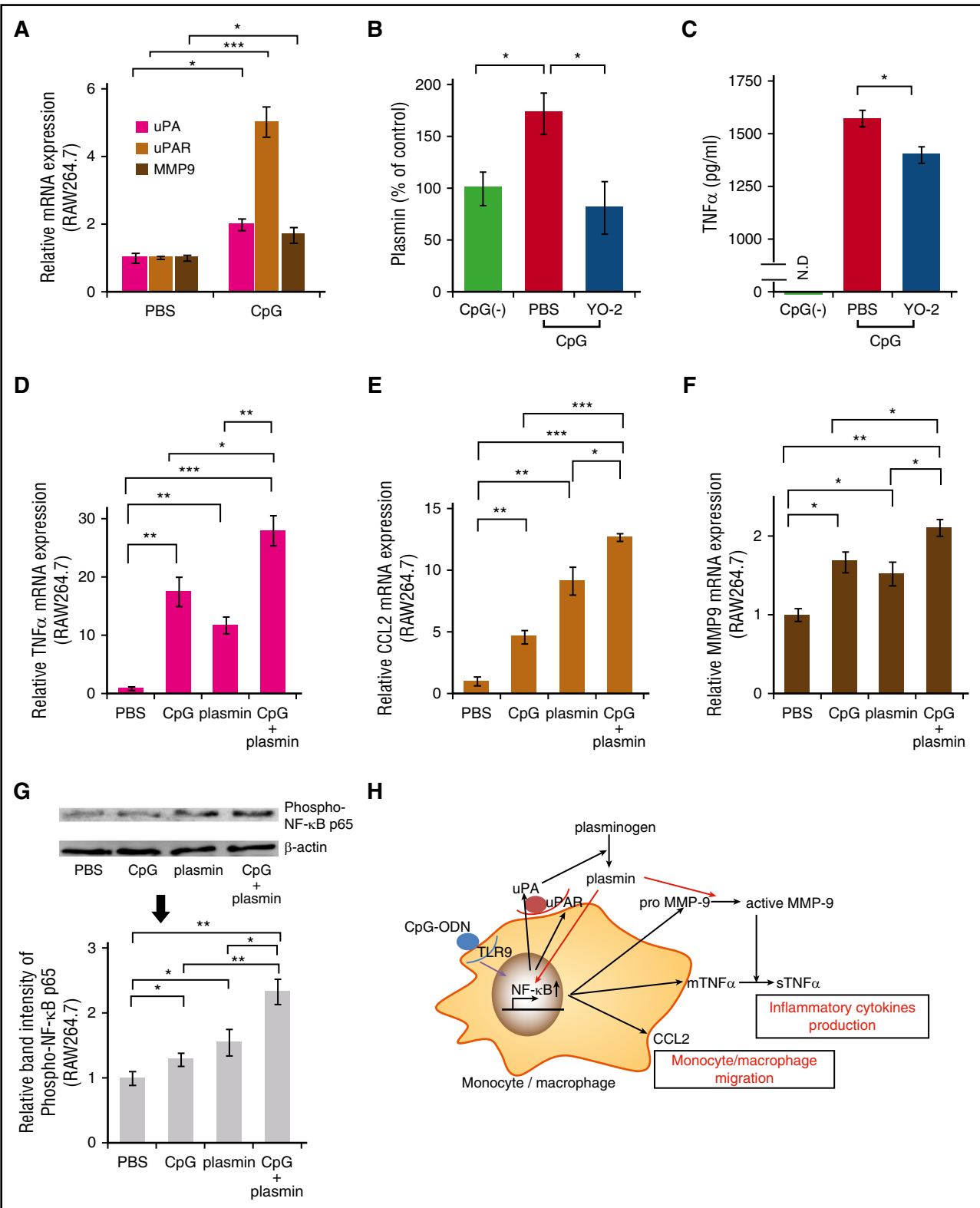


**Figure 7. TLR-9 stimulation leads to the activation of plasminogen/plasmin and MMP-9 with the activation of NF-κB signaling in macrophages.** (A) Gene expression of uPA, uPAR, and MMP9 in RAW264.7 cells stimulated with CpG for 3 hours was determined by quantitative PCR (qPCR) (n = 3 per group). (B) RAW264.7 cells pretreated with PBS or YO-2 were stimulated with CpG for 3 hours. Culture supernatants were assayed for plasmin (n = 3 per group). (C) RAW264.7 cells pretreated with PBS or YO-2 were stimulated with CpG for 8 hours. TNF-α levels were determined using ELISA (n = 3 per group). (D-F) RAW264.7 cells were stimulated with plasmin, CpG, or plasmin/CpG for 3 hours. The gene expression of (D) TNF-α, (E) CCL2, and (F) MMP-9 in cultured cells was determined by qPCR (n = 3 per group). (G) Western blot of phosphorylated-NF-κB p65 in RAW264.7 cells stimulated with plasmin, CpG, or plasmin/CpG for 30 minutes (n = 3 per group). (H) Proposed mechanism by which plasmin enhances the cytokine storm in MAS. Data represent mean ± SEM. \*P < .05, \*\*P < .01, \*\*\*P < .001, using 1-way ANOVA with the Tukey posttest or the unpaired, 2-tailed Student *t* test for significance. mRNA, messenger RNA; mTNF, membrane TNF-α; sTNF, soluble TNF-α.

model can trigger a severe inflammation response with augmented macrophage and neutrophil recruitment that leads to death in the animals.

We showed that pharmacological rather than genetic ablation of plasminogen/plasmin prevented MAS-like symptoms better. The reason for that might lay in the differences in the fibrin deposition and the fibrin-associated inflammatory response. Further studies on the role of fibrinogen will be necessary to address the involvement of fibrin/fibrinogen in MAS progression.

### Plasmin activation due to TLR-9 stimulation can drive the cytokine storm

We confirmed the previous reports by others<sup>44,46,52</sup> showing that TLR-9 stimulation enhanced NF- $\kappa$ B signaling in macrophages leading to augmented expression of NF- $\kappa$ B downstream target genes like TNF- $\alpha$ , CCL2, uPA, and uPAR. Increased plasmin activity was found in supernatants of TLR-9-stimulated macrophages in vitro, most likely due to enhanced expression of uPA and uPAR in these cells. Similarly, increased plasma levels of PAP and uPA were found in CpG/DG-injected mice. As already reported, plasmin-induced activation of the NF- $\kappa$ B pathway increases TNF- $\alpha$  and CCL2 gene expression in monocytes/macrophages.<sup>13,16,40</sup> Our findings are consistent with the results by others showing that CpG-induced MMP-9 expression required TLR-9-dependent activation of NF- $\kappa$ B.<sup>53</sup> Interestingly, TLR-9 stimulation enhanced NF- $\kappa$ B activation in synergy with plasmin, a phenomena already reported for TLR-4.<sup>45</sup> The synergism observed between TLR-4 and plasmin observed in macrophages did not depend on protease-activated receptors 1 or 2, but required the catalytic activity of plasmin. We speculate that plasmin-mediated TLR-4 and TLR-9 signal potentiation might be due to modification of the activity of protein targets in monocytes. We observed higher TNF- $\alpha$  gene expression in TLR-9-activated macrophages. Our data suggest an amplification loop of TNF- $\alpha$  that, through the generation of more plasmin, maintains NF- $\kappa$ B activation and TNF- $\alpha$  upregulation in vivo. But further studies will be necessary to curtail the underlying mechanism.

Plasmin can alter TNF- $\alpha$  and Fas-L activity at the posttranslational level via proteases by a process called shedding. MMP inhibitors can also block the processing of TNF- $\alpha$  and Fas-L.<sup>49,54-56</sup> Lower TNF-plasma levels were found in MAS-induced *Mmp9*<sup>-/-</sup> mice.<sup>4</sup> Our present data are in line with murine inflammatory disease models, where plasmin had been shown to activate MMP-9.<sup>3,4</sup> These data indicate that plasmin inhibition controls cytokine/chemokine production by blocking both their transcription and processing.

### Plasmin enhances monocyte/macrophage infiltration into tissues

During infection and inflammation, CCL2-CCR2 signaling is important for inflammatory monocyte mobilization from the BM to the periphery.<sup>57,58</sup> We showed that plasmin inhibition reduced CCL2 production in CpG/DG-injected mice and suppressed the increase of CCR2<sup>+</sup> cells in the spleen. CpG injection mobilizes inflammatory monocytes to the periphery, where they differentiate into monocyte-derived dendritic cells and can engulf erythroid cells.<sup>47</sup> Our results expand these data by showing that plasmin, by the production of chemokines such as CCL2, enhances this mobilization of inflammatory monocytes and their infiltration into target organs.

### Plasmin inhibition leads to reduction of inflammatory cytokines like TNF- $\alpha$

Plasmin inhibition could not alter elevated IFN- $\gamma$  in CpG/DG-induced MAS, but improved anemia. The amelioration of anemia, but not thrombocytopenia or leukopenia, in *Plg*<sup>-/-</sup> mice and YO-2-treated

mice suggests that plasmin-dependent effects on peripheral cellularity were unique to the erythroid line. TNF- $\alpha$  and Fas-L can suppress erythropoiesis through TNF-R1 or Fas signaling, respectively.<sup>59</sup> Plasmin inhibition attenuated the increase of plasma Fas-L and TNF- $\alpha$  levels in CpG/DG-induced MAS and prevented splenic erythroblast apoptosis. Our data indicate that plasmin inhibition ameliorates anemia in CpG/DG-induced MAS mice through the reduction of inflammatory cytokines.

IFN- $\gamma$  promotes hemophagocytosis.<sup>60-62</sup> IFN- $\gamma$  stimulation leads to plasmin activation in monocytes/macrophages through the activation of uPA/uPAR.<sup>63</sup> We showed that plasma IFN- $\gamma$  elevation was not changed after YO-2 treatment in CpG/DG-injected mice. Conversely, IFN- $\gamma$  production can enhance plasminogen activator secretion from macrophages generating more plasmin.<sup>3</sup> We suggest that blockade of IFN- $\gamma$  may also be effective in CpG/DG-induced MAS due to this feedback mechanism, but further studies will need to show that.

### Plasmin inhibition ameliorates the fatal cytokine storm

We found that plasmin was excessively activated during the first 4 days after the onset of CpG/DG-induced MAS. Consistent with this, YO-2 treatment was most effective given within the first 4 days. There is an important therapeutic window to benefit from plasmin inhibition in the treatment of MAS. In summary, we report that TLR-9 activation upregulates fibrinolytic factors and MMP-9 in myeloid cells, like macrophages, in part by enhancing NF- $\kappa$ B signaling. This proteolytic environment controls cellular infiltration and the production and secretion of proinflammatory cytokines and chemokines. Although plasmin is well known to dissolve fibrin clots, our data suggest that the excessive production of plasmin can enhance the inflammatory response in MAS. Targeting plasmin can suppress the MMP cascade, thereby controlling the release of several proinflammatory cytokines. Plasmin inhibition may be a useful treatment in the prevention of inflammatory processes during MAS progression.

## Acknowledgments

The authors thank Robert Whittier, Lin Shiou-Yuh, and Kengo Shibata for proofreading the manuscript.

This work was supported by grants from the Japan Society for the Promotion of Science (Kiban C grant no. 16K09821 [B.H.]; grant no. 26461415 [K.H.]; grant no. 15K21373 [Y. Tashiro]), and Grants-in-Aid for Scientific Research from the Ministry of Education, Culture, Sports, Science and Technology (grant no. 18013021 [B.H.]), a Grant-in-Aid for Scientific Research on Innovative Areas (grant no. 22112007 [B.H.]), Health and Labor Sciences Research Grants (grant no. 24 008 [K.H.]), and a Naito Grant (B.H.).

## Authorship

Contribution: H.S., B.H., and K.H. designed and performed the experiments, analyzed the data, and wrote the manuscript; Y.S., Y. Ota, and H.O. participated in performing certain experiments; S.M., Y. Tashiro, D.D., and S.E. participated in discussions; Y. Tsuda and Y. Okada provided reagents; and H.N. gave technical support.

Conflict-of-interest disclosure: The authors declare no competing financial interests.

Correspondence: Beate Heissig, Division of Stem Cell Dynamics, Center for Stem Cell Biology and Regenerative Medicine, The Institute of Medical Science, The University of Tokyo, 4-6-1, Shirokanedai, Minato-ku, Tokyo 108-8639, Japan; e-mail: heissig@ims.u-tokyo.ac.jp.



## References

- Janka GE. Familial and acquired hemophagocytic lymphohistiocytosis. *Eur J Pediatr*. 2007;166(2):95-109.
- Janka GE, Lehmborg K. Hemophagocytic syndromes—an update. *Blood Rev*. 2014;28(4):135-142.
- Sato A, Nishida C, Sato-Kusubata K, et al. Inhibition of plasmin attenuates murine acute graft-versus-host disease mortality by suppressing the matrix metalloproteinase-9-dependent inflammatory cytokine storm and effector cell trafficking. *Leukemia*. 2015;29(1):145-156.
- Munakata S, Tashiro Y, Nishida C, et al. Inhibition of plasmin protects against colitis in mice by suppressing matrix metalloproteinase 9-mediated cytokine release from myeloid cells. *Gastroenterology*. 2015;148(3):565-578.e4.
- Loscalzo J. The macrophage and fibrinolysis. *Semin Thromb Hemost*. 1996;22(6):503-506.
- Rao CN, Mohanam S, Puppala A, Rao JS. Regulation of ProMMP-1 and ProMMP-3 activation by tissue factor pathway inhibitor-2/matrix-associated serine protease inhibitor. *Biochem Biophys Res Commun*. 1999;255(1):94-98.
- Knäuper V, Will H, López-Otin C, et al. Cellular mechanisms for human procollagenase-3 (MMP-13) activation. Evidence that MT1-MMP (MMP-14) and gelatinase A (MMP-2) are able to generate active enzyme. *J Biol Chem*. 1996;271(29):17124-17131.
- Ramos-DeSimone N, Hahn-Dantona E, Siple J, Nagase H, French DL, Quigley JP. Activation of matrix metalloproteinase-9 (MMP-9) via a converging plasmin/stromelysin-1 cascade enhances tumor cell invasion. *J Biol Chem*. 1999;274(19):13066-13076.
- Janka GE. Hemophagocytic syndromes. *Blood Rev*. 2007;21(5):245-253.
- Hasegawa D, Kojima S, Tatsumi E, et al. Elevation of the serum Fas ligand in patients with hemophagocytic syndrome and Diamond-Blackfan anemia. *Blood*. 1998;91(8):2793-2799.
- Henter JI, Eliander G, Söder O, Hansson M, Andersson B, Andersson U. Hypercytokinemia in familial hemophagocytic lymphohistiocytosis. *Blood*. 1991;78(11):2918-2922.
- Cauwe B, Opendakker G. Intracellular substrate cleavage: a novel dimension in the biochemistry, biology and pathology of matrix metalloproteinases. *Crit Rev Biochem Mol Biol*. 2010;45(5):351-423.
- Syrovets T, Jendrach M, Rohwedder A, Schüle A, Simmet T. Plasmin-induced expression of cytokines and tissue factor in human monocytes involves AP-1 and IKK $\beta$ -mediated NF- $\kappa$ B activation. *Blood*. 2001;97(12):3941-3950.
- Li Q, Verma IM. NF- $\kappa$ B regulation in the immune system. *Nat Rev Immunol*. 2002;2(10):725-734.
- Collen D. Ham-Wasserman lecture: role of the plasminogen system in fibrin-homeostasis and tissue remodeling. *Hematology Am Soc Hematol Educ Program*. 2001;2001:1-9.
- Burysek L, Syrovets T, Simmet T. The serine protease plasmin triggers expression of MCP-1 and CD40 in human primary monocytes via activation of p38 MAPK and janus kinase (JAK)/STAT signaling pathways. *J Biol Chem*. 2002;277(36):33509-33517.
- Ohki M, Ohki Y, Ishihara M, et al. Tissue type plasminogen activator regulates myeloid-cell dependent neovascularization during tissue regeneration. *Blood*. 2010;115(21):4302-4312.
- Tashiro Y, Nishida C, Sato-Kusubata K, et al. Inhibition of PAI-1 induces neutrophil-driven neovascularization and promotes tissue regeneration via production of angiocrine factors in mice. *Blood*. 2012;119(26):6382-6393.
- Gong Y, Hart E, Shchurin A, Hoover-Plow J. Inflammatory macrophage migration requires MMP-9 activation by plasminogen in mice. *J Clin Invest*. 2008;118(9):3012-3024.
- Carmo AA, Costa BR, Vago JP, et al. Plasmin induces in vivo monocyte recruitment through protease-activated receptor-1-, MEK/ERK-, and CCR2-mediated signaling. *J Immunol*. 2014;193(7):3654-3663.
- Strippoli R, Carvello F, Scianaro R, et al. Amplification of the response to Toll-like receptor ligands by prolonged exposure to interleukin-6 in mice: implication for the pathogenesis of macrophage activation syndrome. *Arthritis Rheum*. 2012;64(5):1680-1688.
- Prahalad S, Bove KE, Dickens D, Lovell DJ, Grom AA. Etanercept in the treatment of macrophage activation syndrome. *J Rheumatol*. 2001;28(9):2120-2124.
- Bruck N, Suttrop M, Kabus M, Heubner G, Gahr M, Pessler F. Rapid and sustained remission of systemic juvenile idiopathic arthritis-associated macrophage activation syndrome through treatment with anakinra and corticosteroids. *J Clin Rheumatol*. 2011;17(1):23-27.
- Sandhu C, Chesney A, Piliotis E, Buckstein R, Koren S. Macrophage activation syndrome after etanercept treatment. *J Rheumatol*. 2007;34(1):241-242.
- Henzan T, Nagafuji K, Tsukamoto H, et al. Success with infliximab in treating refractory hemophagocytic lymphohistiocytosis. *Am J Hematol*. 2006;81(1):59-61.
- Makay B, Yilmaz S, Türkyilmaz Z, Unal N, Oren H, Unsal E. Etanercept for therapy-resistant macrophage activation syndrome. *Pediatr Blood Cancer*. 2008;50(2):419-421.
- Liu J, Guo YM, Onai N, et al. Cytosine-phosphorothionate-guanine oligodeoxynucleotides exacerbates hemophagocytosis by inducing tumor necrosis factor- $\alpha$  production in mice after bone marrow transplantation. *Biol Blood Marrow Transplant*. 2016;22(4):627-636.
- Ramanan AV, Schneider R. Macrophage activation syndrome following initiation of etanercept in a child with systemic onset juvenile rheumatoid arthritis. *J Rheumatol*. 2003;30(2):401-403.
- Fitzgerald AA, Leclercq SA, Yan A, Homik JE, Dinarello CA. Rapid responses to anakinra in patients with refractory adult-onset Still's disease. *Arthritis Rheum*. 2005;52(6):1794-1803.
- Miettunen PM, Narendran A, Jayanthan A, Behrens EM, Cron RQ. Successful treatment of severe paediatric rheumatic disease-associated macrophage activation syndrome with interleukin-1 inhibition following conventional immunosuppressive therapy: case series with 12 patients. *Rheumatology (Oxford)*. 2011;50(2):417-419.
- Nigrovic PA, Mannion M, Prince FH, et al. Anakinra as first-line disease-modifying therapy in systemic juvenile idiopathic arthritis: report of forty-six patients from an international multicenter series. *Arthritis Rheum*. 2011;63(2):545-555.
- Behrens EM, Canna SW, Slade K, et al. Repeated TLR9 stimulation results in macrophage activation syndrome-like disease in mice. *J Clin Invest*. 2011;121(6):2264-2277.
- Yi AK, Yoon H, Park JE, Kim BS, Kim HJ, Martinez-Hernandez A. CpG DNA-mediated induction of acute liver injury in D-galactosamine-sensitized mice: the mitochondrial apoptotic pathway-dependent death of hepatocytes. *J Biol Chem*. 2006;281(21):15001-15012.
- Maes M, Vinken M, Jaeschke H. Experimental models of hepatotoxicity related to acute liver failure. *Toxicol Appl Pharmacol*. 2016;290:86-97.
- Heissig B, Hattori K, Dias S, et al. Recruitment of stem and progenitor cells from the bone marrow niche requires MMP-9 mediated release of kit-ligand. *Cell*. 2002;109(5):625-637.
- Lee E, Enomoto R, Takemura K, Tsuda Y, Okada Y. A selective plasmin inhibitor, trans-aminomethylcyclohexanecarbonyl-L-(O-picolyl) tyrosine-octylamide (YO-2), induces thymocyte apoptosis. *Biochem Pharmacol*. 2002;63(7):1315-1323.
- Bugge TH, Flick MJ, Daugherty CC, Degen JL. Plasminogen deficiency causes severe thrombosis but is compatible with development and reproduction. *Genes Dev*. 1995;9(7):794-807.
- Hald A, Rønne B, Melander MC, Ding M, Holck S, Lund LR. MMP9 is protective against lethal inflammatory mass lesions in the mouse colon. *Dis Model Mech*. 2011;4(2):212-227.
- Dhahri D, Sato-Kusubata K, Ohki-Koizumi M, et al. Fibrinolytic crosstalk with endothelial cells expands murine mesenchymal stromal cells. *Blood*. 2016;128(8):1063-1075.
- Li Q, Laumonier Y, Syrovets T, Simmet T. Plasmin triggers cytokine induction in human monocyte-derived macrophages. *Arterioscler Thromb Vasc Biol*. 2007;27(6):1383-1389.
- de Jager W, Hoppenreijns EP, Wulffraat NM, Wedderburn LR, Kuis W, Prakken BJ. Blood and synovial fluid cytokine signatures in patients with juvenile idiopathic arthritis: a cross-sectional study. *Ann Rheum Dis*. 2007;66(5):589-598.
- Sheehan JJ, Zhou C, Gravanis I, et al. Proteolytic activation of monocyte chemoattractant protein-1 by plasmin underlies excitotoxic neurodegeneration in mice. *J Neurosci*. 2007;27(7):1738-1745.
- Roelofs JJ, Rouschop KM, Leemans JC, et al. Tissue-type plasminogen activator modulates inflammatory responses and renal function in ischemia reperfusion injury. *J Am Soc Nephrol*. 2006;17(1):131-140.
- Takeshita F, Gursel I, Ishii KJ, Suzuki K, Gursel M, Klinman DM. Signal transduction pathways mediated by the interaction of CpG DNA with Toll-like receptor 9. *Semin Immunol*. 2004;16(1):17-22.
- Ward JR, Dower SK, Whyte MK, Buttle DJ, Sabroe I. Potentiation of TLR4 signalling by plasmin activity. *Biochem Biophys Res Commun*. 2006;341(2):299-303.
- Gum R, Lengyel E, Juarez J, et al. Stimulation of 92-kDa gelatinase B promoter activity by ras is mitogen-activated protein kinase kinase 1-independent and requires multiple transcription factor binding sites including closely spaced PEA3/ets and AP-1 sequences. *J Biol Chem*. 1996;271(18):10672-10680.
- Ohyagi H, Onai N, Sato T, et al. Monocyte-derived dendritic cells perform hemophagocytosis to fine-tune excessive immune responses. *Immunity*. 2013;39(3):584-598.
- Koj A, Dubin A. The effect of D-galactosamine on plasma protein synthesis by the perfused rat liver from turpentine-stimulated donors. *Br J Exp Pathol*. 1978;59(5):504-513.
- Bajou K, Peng H, Laug WE, et al. Plasminogen activator inhibitor-1 protects endothelial cells from

- FasL-mediated apoptosis. *Cancer Cell*. 2008; 14(4):324-334.
50. Bezerra JA, Bugge TH, Melin-Aldana H, et al. Plasminogen deficiency leads to impaired remodeling after a toxic injury to the liver. *Proc Natl Acad Sci USA*. 1999;96(26):15143-15148.
51. Bugge TH, Kombrinck KW, Flick MJ, Daugherty CC, Danton MJ, Degen JL. Loss of fibrinogen rescues mice from the pleiotropic effects of plasminogen deficiency. *Cell*. 1996;87(4): 709-719.
52. Wang Y, Dang J, Wang H, Allgayer H, Murrell GA, Boyd D. Identification of a novel nuclear factor-kappaB sequence involved in expression of urokinase-type plasminogen activator receptor. *Eur J Biochem*. 2000;267(11):3248-3254.
53. Lim EJ, Lee SH, Lee JG, et al. Toll-like receptor 9 dependent activation of MAPK and NF-kB is required for the CpG ODN-induced matrix metalloproteinase-9 expression. *Exp Mol Med*. 2007;39(2):239-245.
54. Gearing AJ, Beckett P, Christodoulou M, et al. Processing of tumour necrosis factor-alpha precursor by metalloproteinases. *Nature*. 1994; 370(6490):555-557.
55. Hattori K, Hirano T, Ushiyama C, et al. A metalloproteinase inhibitor prevents lethal acute graft-versus-host disease in mice. *Blood*. 1997; 90(2):542-548.
56. McGeehan GM, Becherer JD, Bast RC Jr, et al. Regulation of tumour necrosis factor-alpha processing by a metalloproteinase inhibitor. *Nature*. 1994;370(6490):558-561.
57. Boring L, Gosling J, Chensue SW, et al. Impaired monocyte migration and reduced type 1 (Th1) cytokine responses in C-C chemokine receptor 2 knockout mice. *J Clin Invest*. 1997;100(10): 2552-2561.
58. Serbina NV, Pamer EG. Monocyte emigration from bone marrow during bacterial infection requires signals mediated by chemokine receptor CCR2. *Nat Immunol*. 2006;7(3):311-317.
59. Testa U. Apoptotic mechanisms in the control of erythropoiesis. *Leukemia*. 2004;18(7):1176-1199.
60. Jordan MB, Hildeman D, Kappler J, Marrack P. An animal model of hemophagocytic lymphohistiocytosis (HLH): CD8+ T cells and interferon gamma are essential for the disorder. *Blood*. 2004;104(3):735-743.
61. Zoller EE, Lykens JE, Terrell CE, et al. Hemophagocytosis causes a consumptive anemia of inflammation. *J Exp Med*. 2011;208(6): 1203-1214.
62. Pachlopnik Schmid J, Ho CH, Chrétien F, et al. Neutralization of IFNgamma defeats haemophagocytosis in LCMV-infected perforin- and Rab27a-deficient mice. *EMBO Mol Med*. 2009;1(2):112-124.
63. Sitrin RG, Todd RF III, Mizukami IF, Gross TJ, Shollenberger SB, Gyetko MR. Cytokine-specific regulation of urokinase receptor (CD87) expression by U937 mononuclear phagocytes. *Blood*. 1994;84(4):1268-1275.